

COMPARISON OF K^* PRODUCTION IN THE REACTIONS $K^+ + n \rightarrow K^+ + \pi^- + p$ AND $K^+ + p \rightarrow K^0 + \pi^+ + p$
AT 2.3 BeV/c*

S. Goldhaber, J. L. Brown, I. Butterworth, G. Goldhaber,
A. A. Hirata, J. A. Kadyk, and G. H. Trilling

Department of Physics and Lawrence Radiation Laboratory, University of California, Berkeley, California

(Received 16 September 1965)

We report here on a study of peripheral K^* production in interactions of K^+ mesons with protons and neutrons:

$$K^+ + n \rightarrow K^+ + \pi^- + p, \quad (1)$$

$$K^+ + p \rightarrow K^0 + \pi^+ + p. \quad (2)$$

We have observed marked differences in the distribution of four-momentum transfer to the K^* and in the K^* decay angular distributions for the two reactions. The results are consistent with production of K^{*0} in Reaction (1) by the exchange of an isovector meson (π), while production of K^{*+} in Reaction (2) largely involves the exchange of an isoscalar meson (ω).

This work is based on an analysis of 100 000 photographs taken with the Brookhaven National Laboratory 20-in. bubble chamber filled with deuterium and exposed in a 2.3-BeV/c K^+ beam at the AGS.¹ The properties of the reactions are deduced, respectively, from events of the type $K^+ + d \rightarrow K^+ + \pi^- + p + p$ and $K^+ + d \rightarrow K^0 + \pi^+ + p + n$. The slower nucleon is defined as the

spectator and is required to have a momentum less than 300 MeV/c. With this limitation the momentum spectrum of the spectator agrees well with that expected from the Hulthén wave function, and its angular distribution in the laboratory system is isotropic. It is thus reasonable to consider our data in terms of the impulse approximation as implied in Reactions (1) and (2).

Our analysis is based on 1576 events of Reaction (1) and 602 events of Reactions (2). The cross sections for these reactions are, respectively, 3.0 ± 0.2 mb and 3.0 ± 0.3 mb.² In Fig. 1 we show the Dalitz plots of $M_{N\pi}^2$ vs $M_{K\pi}^2$ for Reactions (1) and (2). Strong K^* production is evident in each case. The cross sections for K^* production in the reactions $K^+ + n \rightarrow p + K^{*0}$ ($K^{*0} \rightarrow K^+ + \pi^-$) and $K^+ + p \rightarrow p + K^{*+}$ ($K^{*+} \rightarrow K^0 + \pi^+$) are 1.4 ± 0.2 mb and 1.3 ± 0.2 mb, respectively. In Figs. 2(a) and 2(d) we show the distribution of the momentum transfer squared, $\Delta_{K\pi}^2$, for events in the respective K^* bands ($0.86 \leq M_{K\pi} \leq 0.96$ BeV).³ The data shown have

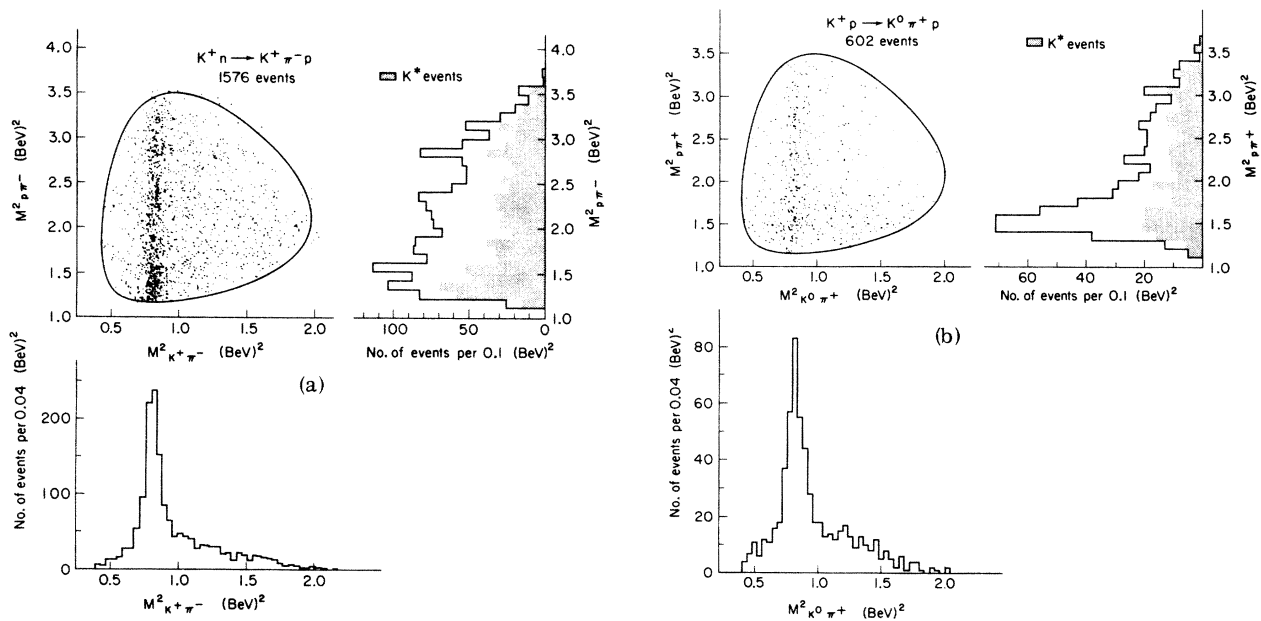


FIG. 1. (a) Dalitz plot for the reaction $K^+ + n \rightarrow K^+ + \pi^- + p$; (b) Dalitz plot for the reaction $K^+ + p \rightarrow K^0 + \pi^+ + p$. The shaded histograms show $M_{K\pi}$ for those events where $M_{K\pi}$ lies in the K^* region, $0.86 \leq M_{K\pi} \leq 0.96$ BeV.

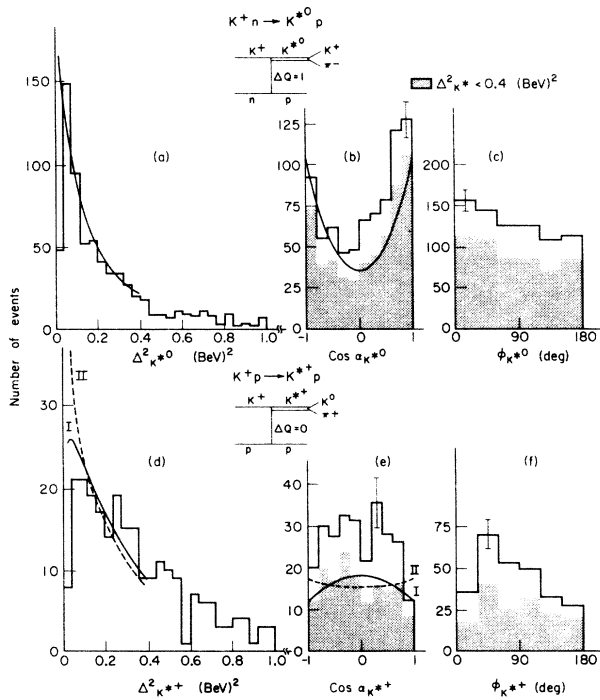


FIG. 2. Comparison of the reactions $K^+ + n \rightarrow K^{*0} + p$ ($K^{*0} \rightarrow K^+ + \pi^-$) and $K^+ + p \rightarrow K^{*+} + p$ ($K^{*+} \rightarrow K^0 + \pi^+$). (a) and (d): Four-momentum transfer to the K^* , plotted up to 1.0 BeV^2 ; (b) and (e): $K\pi$ scattering angle, α_{K^*} , in $K\pi$ c.m. system; (c) and (f): Treiman-Yang angle ϕ_{K^*} . Shaded histograms show angular distributions for events with $\Delta_{K\pi}^2 \leq 0.4 \text{ BeV}^2$. The curves show the results of absorption-model calculations by Jackson *et al.*⁷ normalized to the data for $\Delta_{K\pi}^2 \leq 0.4 \text{ BeV}^2$.

not been corrected for background effects. The shapes are not noticeably changed, however, by such corrections. The distributions are markedly different, that for K^{*+} production being much broader than that for K^{*0} . The distributions of the $K\pi$ scattering angle, $\cos\alpha_{K\pi}$, in the K^* center-of-mass system [Figs. 2(b) and 2(e)] and of the Treiman-Yang angle, ϕ [Figs. 2(c) and 2(f)], are shown for events in the K^* band. The shaded region corresponds to events with $\Delta_{K\pi}^2 \leq 0.4 \text{ (BeV)}^2$.⁴ Here again a marked difference between the two reactions is seen, particularly in the $\cos\alpha_{K\pi}$ distributions. That for K^{*0} production has a large $\cos^2\alpha$ term indicative of a dominant π -exchange production process, while that for K^{*+} production is predominantly isotropic with a small $\sin^2\alpha$ contribution suggesting that vector exchange is of importance here. We note that K^{*0} production in Reaction (1) requires the exchange of an isovector meson and could proceed via

π or ρ exchange or both, whereas the K^{*+} production in Reaction (2) requires the exchange of a neutral meson and could proceed via the exchange of one or more of the mesons π , ρ , ω , and ϕ . Our experimental results, discussed above, indicate that different exchange particles dominate the two reactions and, furthermore, that ρ exchange is strongly suppressed in Reaction (1), where one would have expected a contribution four times as large as in Reaction (2). This leads us to the conclusion that isoscalar exchange must play an important part in Reaction (2), and that ρ exchange appears to be suppressed in K^* production. If the Bronzan-Low quantum number is valid, it provides an interpretation of the suppression of the ρ -meson exchange.⁵ Furthermore, this selection rule would suggest suppression of ϕ exchange as well, leaving the ω as the isoscalar exchange meson for Reaction (2).

A quantitative analysis of the decay distribution is complicated by the presence of isobar production in the two reactions. The difficulties are seen most clearly in Reaction (1). The isobars $N_{3/2}^{*0}(1238)$, $N_{1/2}^{*0}(1512)$, and $N_{1/2}^{*0}(1688)$ may be present in our data, but they are not clearly resolved in the over-all $M^2(p\pi^-)$ distribution [Fig. 1(a)]. If $M_{K^+\pi^-}$ is chosen to be in the K^* band, on the other hand (inner histogram of the $M_{p\pi^-}^2$ projection), the $N_{3/2}^{*0}(1238)$ appears strongly. In fact, it is seen from the Dalitz plot that the $N^{*0}(1238)$ is produced predominantly in the K^* band, indicative of constructive interference between the reactions $K^+ + n \rightarrow K^{*0} + p$ and $K^+ + n \rightarrow K^+ + N^{*0}(1238)$. In the three-particle final state, $\cos\alpha_{K\pi}$ and $M_{p\pi^-}$ are correlated. The enhancement in the overlap region of the two resonance bands may thus be the cause of the forward excess in the decay angular distribution, $\cos\alpha_{K\pi}$, shown in Fig. 2(b). Alternatively, one can argue that the forward peaking of the $\cos\alpha_{K\pi}$ distribution is responsible for the apparent constructive interference. However, no such marked decay asymmetry for the K^{*0} is observed in the reaction leading to four particles in the final state $K^+ + p \rightarrow K^{*0} + N^{*++}$.⁶

The theoretical curves shown in Fig. 2 have been calculated by Jackson *et al.*⁷ taking into account effects due to absorption. These curves are normalized to our data for $\Delta_{K\pi}^2 \leq 0.4 \text{ BeV}^2$.⁸ For K^{*0} production only the pion-exchange process is included in the calculation. The curves shown for the K^{*+} events include a π -exchange

Table I. Spin-density matrix element for K^* production in Reactions (1) and (2).^a

Reaction	$\Delta_{K\pi}^2$	ρ_{00}	ρ_{11}	$\text{Re}\rho_{10}$
$K^+ + n \rightarrow K^{*0} + p$	$\Delta_{K\pi}^2 \leq 0.1 \text{ BeV}^2$	$0.55^{+0.08}_{-0.10}$	$-0.02^{+0.08}_{-0.06}$	-0.13 ± 0.05
$\quad \quad \quad \downarrow \quad K^+ + \pi^-$	$0.1 < \Delta_{K\pi}^2 \leq 0.3 \text{ BeV}^2$	$0.75^{+0.05}_{-0.10}$	$-0.02^{+0.08}_{-0.06}$	-0.28 ± 0.04
	$0.3 < \Delta_{K\pi}^2 \leq 1.0 \text{ BeV}^2$	$0.46^{+0.09}_{-0.12}$	$0.0^{+0.1}_{-0.07}$	-0.18 ± 0.05
$K^+ + p \rightarrow K^{*+} + p$	$\Delta_{K\pi}^2 \leq 0.3 \text{ BeV}^2$	$0.31^{+0.08}_{-0.11}$	$0.04^{+0.11}_{-0.08}$	-0.06 ± 0.06
$\quad \quad \quad \downarrow \quad K^0 + \pi^+$	$0.3 < \Delta_{K\pi}^2 \leq 1.0 \text{ BeV}^2$	$0.01^{+0.10}_{-0.12}$	$0.17^{+0.12}_{-0.07}$	-0.09 ± 0.06

^aThe figures given are corrected for background by subtracting the angular distributions for events in the adjacent strips from those for the K^* strip. The corrected values are shifted from the uncorrected ones by an amount no greater than the quoted errors.

term and a large vector-exchange term which may involve vector and tensor coupling constants at the nucleon vertex. From charge independence, pion exchange must also be present in K^{*+} production. The Clebsch-Gordan coefficients, however, reduce its contribution compared with Reaction (1) by a factor of four. The relative strengths of the two vector-exchange couplings are not known a priori. Jackson et al. obtained a good fit to K^{*+} production at 3 BeV/c,⁹ with two different sets of values for the vector and tensor coupling constants. The two curves shown in Figs. 2(d) and 2(e) correspond to the solutions for the two sets of values. In this experiment solution I appears to be a reasonable fit to the data; solution II is less acceptable. The broad features of our experimental distributions agree well with the theoretical curves.

Finally, we have also evaluated the components of the spin-density matrix for the two reactions for which we have forced symmetrical solutions to the decay distributions. The values are shown in Table I.

As may be noted from Table I, the real part of ρ_{10} for Reaction (1) is quite large, which is indicative of the presence of processes other than the simple meson-exchange diagrams. Because of the observed asymmetries in the $\cos\alpha$ distribution, the description of the processes in terms of the density-matrix formalism is not complete. We have therefore further examined the correlations between $\cos\alpha$ and ϕ . In Fig. 3 we show these correlations for

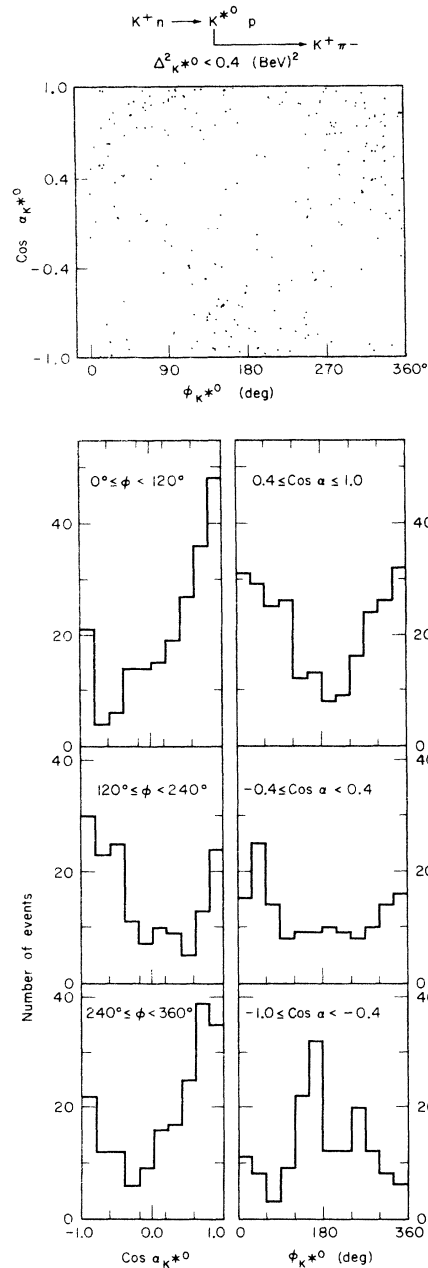


FIG. 3. Correlations between $\cos\alpha_{K^*}$ and ϕ_{K^*} for the reaction $K^+ + n \rightarrow K^{*0} + p$ ($K^{*0} \rightarrow K^+ + \pi^-$). Shown are the scatter plot of $\cos\alpha_{K^*}$ vs ϕ_{K^*} , the distribution of $\cos\alpha_{K^*}$ for different regions of ϕ_{K^*} , and the distribution of ϕ_{K^*} for different region of $\cos\alpha_{K^*}$, as indicated.

Reaction (1), which is dominated by pion exchange. These correlations, which are to some extent reflected by the value of $\text{Re}\rho_{10}$, indicate that more complicated processes, in addition to the dominant simple particle exchange, are present in these peripheral collisions.

We are grateful to R. Shutt and his co-workers at the Brookhaven National Laboratory for making available the 20-in. bubble chamber, to the AGS crew, to the 20-in. bubble chamber crew, and particularly to H. Brown for help with the exposure at the AGS. We would like to thank all the many people at Berkeley who helped with scanning, measuring, and computing. Finally, we would like to acknowledge the help of Thomas A. O'Halloran and Benjamin C. Shen, who participated in the early stages of this work.

*This work was done under the auspices of the U. S. Atomic Energy Commission.

¹C. Baltay, J. Sandweiss, J. Sanford, H. Brown, M. Webster, and S. Yamamoto, Nucl. Instr. Methods **20**, 37 (1963).

²Corrections have been made for neutral K^0 decays, and normalization is to 344 τ decays observed in the sample of film used to deduce cross sections (about 60% of the total). There is some uncertainty as to what proportion of the 8% of events with spectators faster than 300 MeV/c should be included in deducing nucleon cross sections. They have been left out completely from the numbers quoted.

³In Reaction (2) there is a slight correction to be considered at small momentum transfers because of the possibility of the recoil proton's recombining with the spectator neutron to form a deuteron. These events have been discussed elsewhere {I. Butterworth, J. L. Brown, G. Goldhaber, S. Goldhaber, A. A. Hirata, J. A. Kadyk, B. M. Schwarzschild, and G. H. Trilling, this issue [Phys. Rev. Letters **15**, 734 (1965)]}. They make a negligibly small change in the distributions discussed here.

⁴The curves are uncorrected for background. Background corrections make little difference; for $\Delta_{K\pi}^2 < 0.4 \text{ BeV}^2$ any effects of background correction are statistically insignificant.

⁵J. B. Bronzan and F. E. Low, Phys. Rev. Letters **12**, 522 (1964).

⁶G. Goldhaber, J. L. Brown, I. Butterworth, S. Goldhaber, A. A. Hirata, J. A. Kadyk, B. C. Shen, and G. H. Trilling, Phys. Letters **18**, 76 (1965).

⁷J. D. Jackson, J. T. Donohue, K. Gottfried, R. Keyser, and B. E. Y. Svensson, Phys. Rev. **139**, B428 (1965).

⁸The K^* production cross sections integrated over the $\Delta_{K\pi}^2$ range 0-0.4 BeV^2 have also been calculated on the absorption model (J. D. Jackson, University of Illinois, private communication). The values obtained are 1.34 mb for the reaction $K^+ + n \rightarrow K^{*0} + p$ ($K^{*0} \rightarrow K^+ + \pi^-$); for the reaction $K^+ + p \rightarrow K^{*+} + p$ ($K^{*+} \rightarrow K^0 + \pi^+$) they are 0.45 and 0.55 mb for solutions I and II, respectively. Our experimental values for this range of momentum transfer are 0.9 ± 0.2 for K^{*0} production and 0.7 ± 0.2 for K^{*+} production.

⁹M. Ferro-Luzzi, R. George, Y. Goldschmidt-Clermont, V. P. Henri, B. Jongejans, D. W. G. Leith, G. R. Lynch, F. Muller, and J. M. Perreau, Nuovo Cimento **36**, 1101 (1965).

E R R A T U M

PHASE CHANGE IN ADSORBED HELIUM AT
LOW TEMPERATURE. D. L. Goodstein, J. G.
Dash, and W. D. McCormick [Phys. Rev. Letters
15, 447 (1965)].

The numerals II and IV in the inset of Fig. 2
should read III and I, respectively.

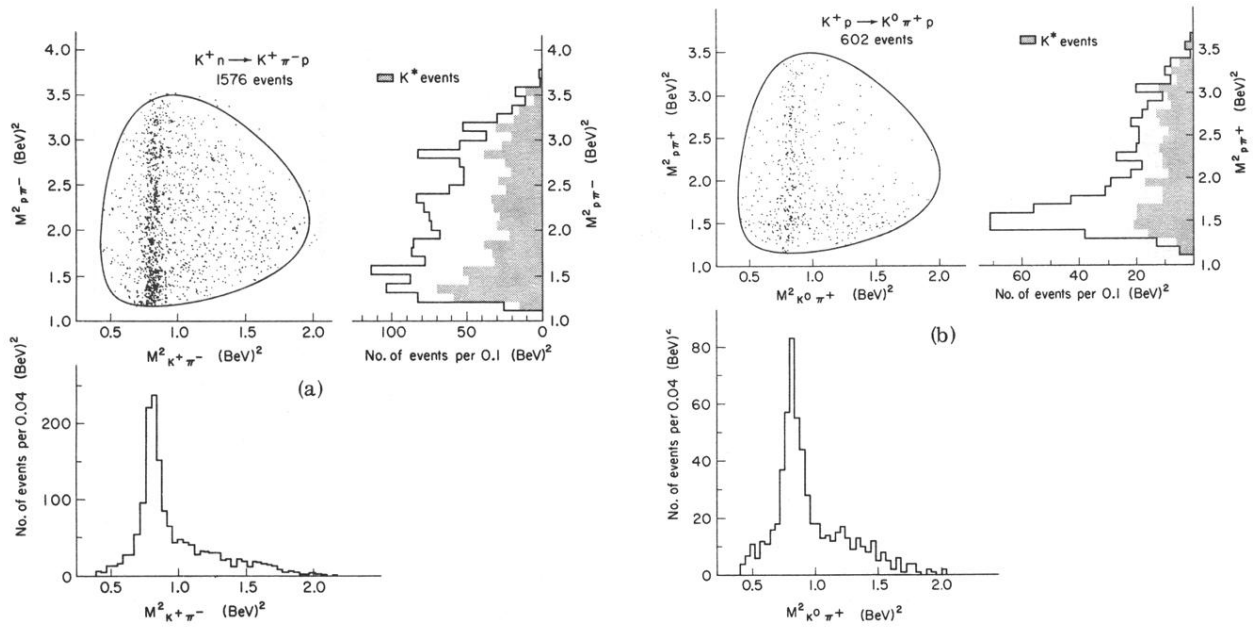


FIG. 1. (a) Dalitz plot for the reaction $K^+ + n \rightarrow K^+ + \pi^- + p$; (b) Dalitz plot for the reaction $K^+ + p \rightarrow K^0 + \pi^- + p$. The shaded histograms show $M_{p\pi}$ for those events where $M_{K\pi}$ lies in the K^* region, $0.86 \leq M_{K\pi} \leq 0.96$ BeV.

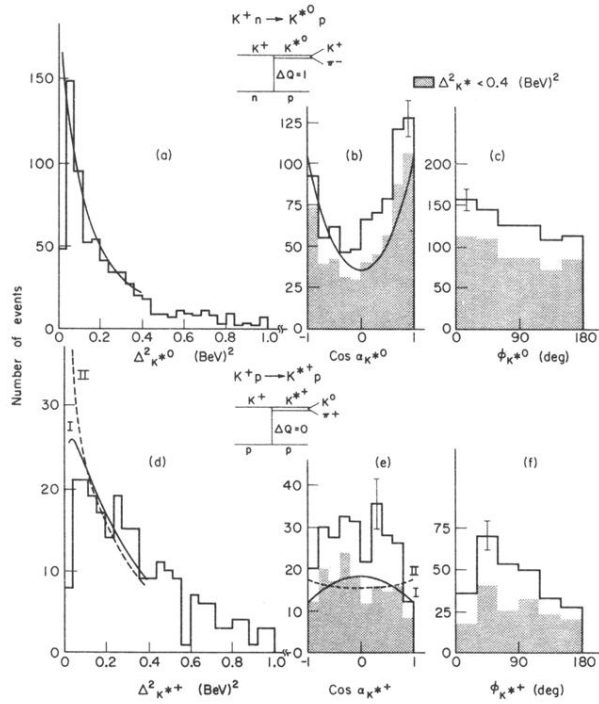


FIG. 2. Comparison of the reactions $K^+ + n \rightarrow K^{*0} + p$ ($K^{*0} \rightarrow K^+ + \pi^-$) and $K^+ + p \rightarrow K^{*+} + p$ ($K^{*+} \rightarrow K^0 + \pi^+$). (a) and (d): Four-momentum transfer to the K^* , plotted up to 1.0 BeV^2 ; (b) and (e): $K\pi$ scattering angle, α_{K^*} , in $K\pi$ c.m. system; (c) and (f): Treiman-Yang angle ϕ_{K^*} . Shaded histograms show angular distributions for events with $\Delta_{K\pi}^2 \leq 0.4 \text{ BeV}^2$. The curves show the results of absorption-model calculations by Jackson *et al.*,⁷ normalized to the data for $\Delta_{K\pi}^2 \leq 0.4 \text{ BeV}^2$.